Distant Effects of a Recurving Tropical Cyclone on Rainfall in a Midlatitude Convective System: A High-Impact Predecessor Rain Event*

RUSS S. SCHUMACHER

National Center for Atmospheric Research,+ Boulder, Colorado, and Department of Atmospheric Sciences, Texas A&M University, College Station, Texas

THOMAS J. GALARNEAU JR.# AND LANCE F. BOSART

Department of Atmospheric and Environmental Sciences, University at Albany, State University of New York, Albany, New York

(Manuscript received 13 April 2010, in final form 30 July 2010)

ABSTRACT

Recent research has identified predecessor rain events (PREs), which are mesoscale regions of heavy rainfall that occur ~1000 km poleward and downshear of recurving tropical cyclones (TCs). PREs typically occur 24–36 h prior to the arrival of the main rain shield associated with the TC, and frequently result in damaging flooding. A distinguishing feature of a PRE is that it is enhanced by a broad region of deep tropical moisture directly associated with the TC that is transported well poleward ahead of the TC. This study will quantify the effects of the tropical moisture from one TC on a record-breaking rain and flood event over the northern Great Plains and southern Great Lakes region on 18–19 August 2007.

In this event, which occurred ahead of TC Erin, a southerly stream of deep tropical moisture (precipitable water values >50 mm) moved poleward and intersected a northwest–southeast-oriented quasi-stationary baroclinic zone beneath the equatorward entrance region of an upper-level jet streak. A slow-moving mesoscale convective system (MCS) developed and produced widespread heavy rainfall, with local amounts exceeding 380 mm that resulted in historic flooding in Minnesota and Wisconsin. Observations and numerical simulations using the Advanced Research Weather Research and Forecasting model (ARW-WRF) indicate that low-level frontogenesis was maximized during the overnight hours of 19 August 2007 and provided the forcing for vigorous ascent during the mature stage of the PRE. A control simulation, which included the poleward transport of TC Erin-related moisture, reproduced the extreme rainfall amounts, although the simulated rainfall was displaced from where it was observed. A sensitivity simulation in which the moisture associated with TC Erin was removed (referred to as ''NOPLUME'') shows reduced convective available potential energy (CAPE) in the inflow region of the PRE and a less vigorous MCS. In all, there was an approximately 50% reduction in the maximum precipitation amount and a 25% reduction in the total precipitation from the control simulation to the NOPLUME run. Or, considered in the context of rainfall enhancement by the Erin-related moisture, there was a near doubling of the maximum amount and a 33% increase in the total rainfall. The extent of these differences underscores the importance of moisture originating from TC Erin in transforming a heavy rain event into a high-impact, record-breaking rain event.

1. Introduction

a. Overview

On 18–19 August 2007, a slow-moving mesoscale convective system (MCS) produced record rainfall over portions of Minnesota and Wisconsin, which led to catastrophic flash flooding. The rainfall from this MCS set a new statewide, all-time record for 24-h rainfall accumulation of 383.5 mm at Hokah, Minnesota. The Minnesota State Climatology Office (2010) estimated the recurrence interval for 24-h rainfall of this magnitude to

* Supplemental information related to this paper is available at the Journals Online Web site: http://dx.doi.org/10.1175/2010MWR3453.s1.

+ The National Center for Atmospheric Research is sponsored by the National Science Foundation.

Current affiliation: CIRES/University of Colorado, Boulder, Colorado.

Corresponding author address: Russ Schumacher, Department of Atmospheric Sciences, Texas A&M University, College Station, TX 77843.
E-mail: russ.schumacher@tamu.edu

DOI: 10.1175/2010MWR3453.1

be over 2000 yr. In addition to this extreme local rainfall amount, there was a widespread swath of rainfall totals exceeding 50 mm that extended from western Minnesota to southern Michigan (Fig. 1). Over the 3-day period 18–20 August, 529.6 mm of rain fell at Houston, Minnesota. This unprecedented rainfall over the relatively complex terrain of the Mississippi River valley in Minnesota and Wisconsin led to devastating flash floods (e.g., Binau 2009) that caused 8 fatalities, 32 injuries, and over $280 million in damage (NCDC 2007).

In a recent study, Galarneau et al. (2010, hereinafter GBS10) argued that this case of extreme rainfall was a prime example of a predecessor rain event (PRE). PREs occur ahead of recurving tropical cyclones (TCs) when deep tropical moisture, with precipitable water (PW) values of more than 50 mm, is transported well poleward of the TC and is forced to ascend when it encounters a low-level baroclinic zone. The event of interest in the present study occurred ahead of TC Erin, which made landfall along the Texas coast on 16 August and slowly recurved northward into Oklahoma by 19 August (Fig. 1). A stream of tropical moisture (with PW exceeding 50 mm) ahead of Erin arrived in the upper Midwest on 19 August, and GBS10 hypothesized that this moisture enhanced the rainfall production by the MCS over Minnesota and Wisconsin, transforming a heavy rain event into a high-impact, record-breaking event. The present study will test this hypothesis and attempt to quantify the effects of the tropical moisture on the rainfall amounts in the Midwest.

b. Background on heavy rainfall from MCSs

In the warm season, MCSs produce a substantial fraction of the rainfall in the vital agricultural areas of the central United States (e.g., Fritsch et al. 1986), but they are also responsible for a majority of flash-flood-inducing extreme rainfall events (e.g., Schumacher and Johnson 2006). Numerous past studies have documented the synoptic and mesoscale conditions in which heavy-rain-producing MCSs develop (e.g., Maddox et al. 1979; Chappell 1986; Doswell et al. 1996; Junker et al. 1999; Schumacher and Johnson 2005). Doswell et al. (1996) proposed an ingredients-based methodology for understanding and forecasting heavy rainfall. Simply, the rainfall total at a given point equals the average rain rate multiplied by the duration of the rain. High rain rates occur when moist air rises and condenses, and when a large fraction of that condensation reaches the ground as rainfall. The duration of rainfall is increased when the precipitating system moves slowly, and when it is organized such that convective cells repeatedly pass over the same area. In the warm season, these ingredients are often brought together by MCSs.

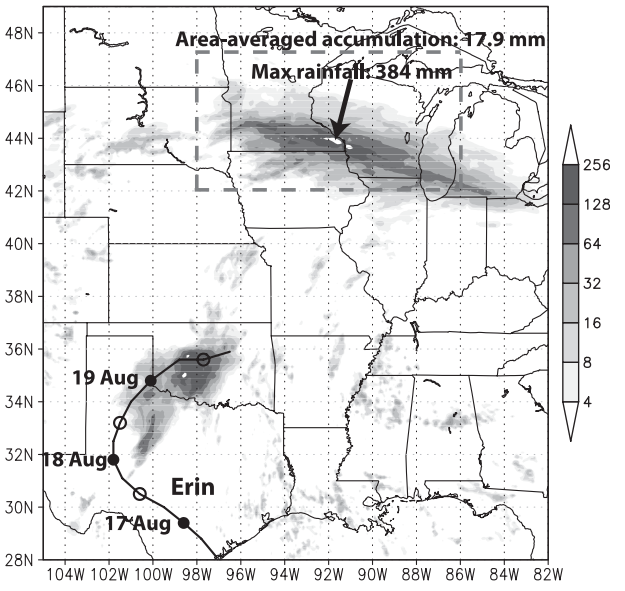

FIG. 1. NCEP stage-IV gridded precipitation analysis (Lin and Mitchell 2005) for the 24-h period 1200 UTC 18 Aug–1200 UTC 19 Aug 2007. Also shown is the National Hurricane Center best track for Erin, with filled circles denoting positions at 0000 UTC and open circles denoting positions at 1200 UTC. The gray dashed rectangle indicates the location of the area-averaged rainfall calculation.

One common location for heavy-rain-producing MCSs is on the cool side of a surface baroclinic zone, when low-level flow perpendicular to the baroclinic zone is forced to ascend, and a linear, elevated MCS develops that is oriented parallel to the boundary. In such situations, the upper-level flow is typically parallel to the baroclinic zone, so individual convective elements move along the boundary but there is little motion across the boundary. These MCSs are most common in the overnight hours (e.g., Maddox et al. 1979; Schumacher and Johnson 2006), in part because a nocturnally enhanced low-level jet (LLJ) transports warm, moist air into the region where the MCS develops, and convergence and warm air advection are enhanced when the LLJ is oriented perpendicular to the boundary. The synoptic and mesoscale conditions leading to this scenario were originally described by Maddox et al. (1979) in their ''frontal'' type of flash flood. Later research by Trier and Parsons (1993) and Augustine and Caracena (1994) demonstrated the processes responsible for initiating and organizing elevated nocturnal MCSs, and Junker et al. (1999) and Moore et al. (2003) synthesized the synoptic and mesoscale environments conducive to these systems. Schumacher and Johnson (2005) described the organization of these linear MCSs as training line/adjoining stratiform (TL/AS), because of the repeated passage of convective cells, known as ''echo training,'' which occurs over locations on the cool side of the boundary.

c. Predecessor rain events

PREs are defined as coherent regions of heavy rainfall occurring well in advance of recurving TCs (GBS10). GBS10 presented a climatology that summarized the key characteristics of PREs through composite analysis of 28 PREs that occurred in the eastern United States during 1995–2008 and an observational case study of the TC Erin PRE. Bosart and Carr (1978) presented what was likely the first in-depth analysis of a PRE in their study of rainfall ahead of TC Agnes (1972). Other more recent studies have described PREs in other parts of the world: Wang et al. (2009) discussed the enhancement of rainfall in Japan ahead of western North Pacific TC Songda (2004), and Stohl et al. (2008) described the transport of tropical moisture all the way to the Norwegian coast at 60°N latitude ahead of two TCs. The event analyzed by Stohl et al. (2008) involved the process typically associated with PREs—a broad region of increased water vapor ahead of a TC—as well as an ''atmospheric river'' (e.g., Zhu and Newell 1998), which differs from most PREs in that it is a very narrow band of increased water vapor.

GBS10 found that a majority of PREs occurred under the equatorward entrance region of an anticyclonically curved 200-hPa jet, downshear of a broad upper-level trough and poleward of an upper-level closed anticyclone. Within such a jet-entrance region, there is quasigeostrophic (QG) forcing for ascent that can contribute to destabilization (e.g., Uccellini and Johnson 1979; Bosart and Lackmann 1995). In the lower troposphere, strong southerly flow was oriented perpendicular to a zonally elongated baroclinic zone, which resulted in strong warm-air advection and frontogenesis at the location of the PRE. Deep tropical moisture was transported poleward ahead of the recurving TC by the strong southerly low-level flow. The forcing for ascent provided by the upper-level jet streak and the low-level frontogenesis, combined with the deep tropical moisture, brought together the necessary ingredients for heavy rainfall (e.g., Doswell et al. 1996).

The purpose of this paper is to quantify the distant effects of tropical moisture ahead of TC Erin on the heavy rainfall in the Midwest on 18–19 August 2007. The remainder of the article is organized as follows. In section 2 of this article, an overview of the event is presented, using observations and model analyses. Section 3 describes a numerical simulation of the event, and section 4 presents a sensitivity simulation in which the plume of moisture associated with Erin is removed. Section 5 presents the conclusions.

2. Overview of the 18–19 August 2007 PRE

A brief analysis of the TC Erin PRE of 18–19 August 2007 is presented here, using observations and operational analyses. For a detailed analysis, the reader is referred to GBS10. As noted by Arndt et al. (2009) and GBS10, TC Erin was a multifaceted high-impact weather event. Erin made landfall along the Texas coast as a weak tropical storm at 1030 UTC 16 August (Brennan et al. 2009; Fig. 1). In addition to the PRE over the Midwest, TC Erin produced heavy rainfall in Texas during 17–19 August, briefly reintensified to tropical storm strength over Oklahoma on 19 August, contributed to an extreme rainfall event in southwestern Missouri on 19–20 August, and triggered a severe weather outbreak over North Carolina and Virginia on 21–22 August (e.g., Schumacher and Johnson 2009; Arndt et al. 2009; GBS10).

The synoptic- and mesoscale pattern at the time of the initiation of the PRE was similar to that shown in the composite of PREs occurring under anticyclonically curved jets shown by GBS10, and is summarized in the schematic diagram in Fig. 2. An upper-level jet streak was located over the northern United States and Canada, with a midlevel anticyclone over the southeastern United States (Fig. 2). The tropical moisture associated with Erin was transported poleward to the upper Midwest by strong southerly and southwesterly low-level winds throughout the Great Plains (Fig. 3). The PW in most of the central United States was more than two standard deviations above the mean, and was more than four standard deviations above the mean near Erin itself (Fig. 3). The preexisting moisture in Minnesota and Iowa was also anomalous, with values more than two standard deviations above the mean at 0000 UTC 19 August 2007 (Fig. 3a), prior to the arrival of the Erin-related moisture between 0000 and 1200 UTC (Figs. 3b,c). This warm, moist air was forced to ascend when it encountered a northwest–southeast-oriented low-level baroclinic zone in the upper Midwest. The frontogenesis along this baroclinic zone was a direct result of confluence between the southerly flow associated with the anticyclone in the southeastern United States and the easterly flow to the north (Figs. 2 and 4a). These processes led to the initiation of an archetypical TL/AS MCS on the cool side of the baroclinic zone in Minnesota and Wisconsin.[1]

Around 2000 UTC 18 August, deep convection initiated on the western edge of a stratiform rain region (the remnant of an MCS from the previous night) in southeastern Minnesota. This convection began to organize into a northwest–southeast-oriented line by 2200 UTC (Fig. 4a). While this convection moved eastward, numerous convective cells initiated on the poleward side of the surface

[1] Animations of reflectivity from radar observations and simulations are available in the online supplement.

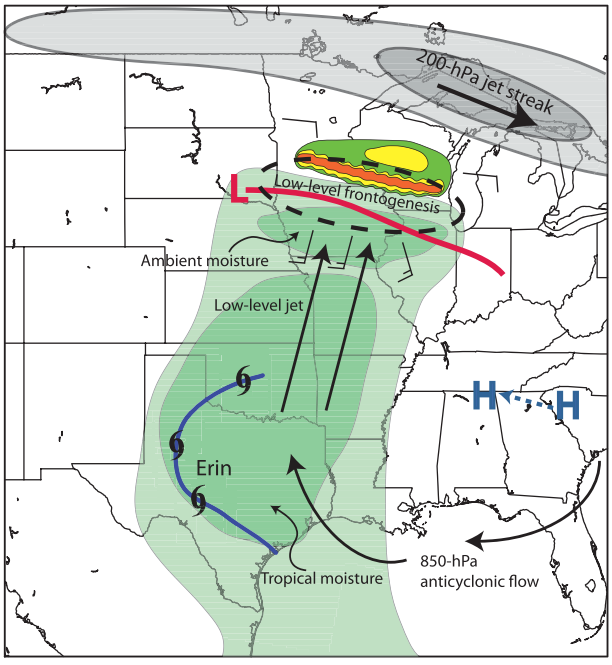

FIG. 2. Schematic diagram showing the primary processes in the TC Erin PRE, and generally representative of a typical PRE occurring under an anticyclonically curved upper-level jet (based on the findings of GBS10). The track of TC Erin and its remnants is shown by the thick blue curve, with the position at 1200 UTC 17 Aug, 18 Aug, and 19 Aug 2007 shown by the TC symbols. The 700-hPa anticyclone, and its movement toward the west-northwest during the event, is shown by the "H" symbols. The surface low pressure center and baroclinic zone are shown by the red "L" and red line, respectively, with the associated low-level frontogenesis maximum outlined in the dashed black line. The 200-hPa isotachs of approximately 30 and 50 m s^{-1} are in gray shading. The 850-hPa flow direction is shown by the black arrows, and some representative surface wind barbs are also shown. Areas of precipitable water greater than 50 (55) mm are shaded in light green (darker green), respectively, and the radar-indicated structure of the extreme-rain-producing MCS is contoured at approximately 20, 40, and 50 dB*Z*.

front across southern Minnesota. By 0300 UTC, a narrow, nearly continuous line of convection extended from the Minnesota–South Dakota border eastward to Lake Michigan (Fig. 4b). This MCS remained essentially stationary between approximately 0000 and 0800 UTC (Fig. 4c), after which it began moving southward and decreasing in intensity. During the time when it had TL/AS structure, individual convective elements moved toward the southeast along the line and new convection repeatedly formed on the west end of the line. In terms of the vector method for describing MCS motion (e.g., Doswell et al. 1996; Corfidi 2003), the cell motion and propagation vectors were approximately equal in magnitude and in opposite directions, yielding an overall system motion that was near zero.

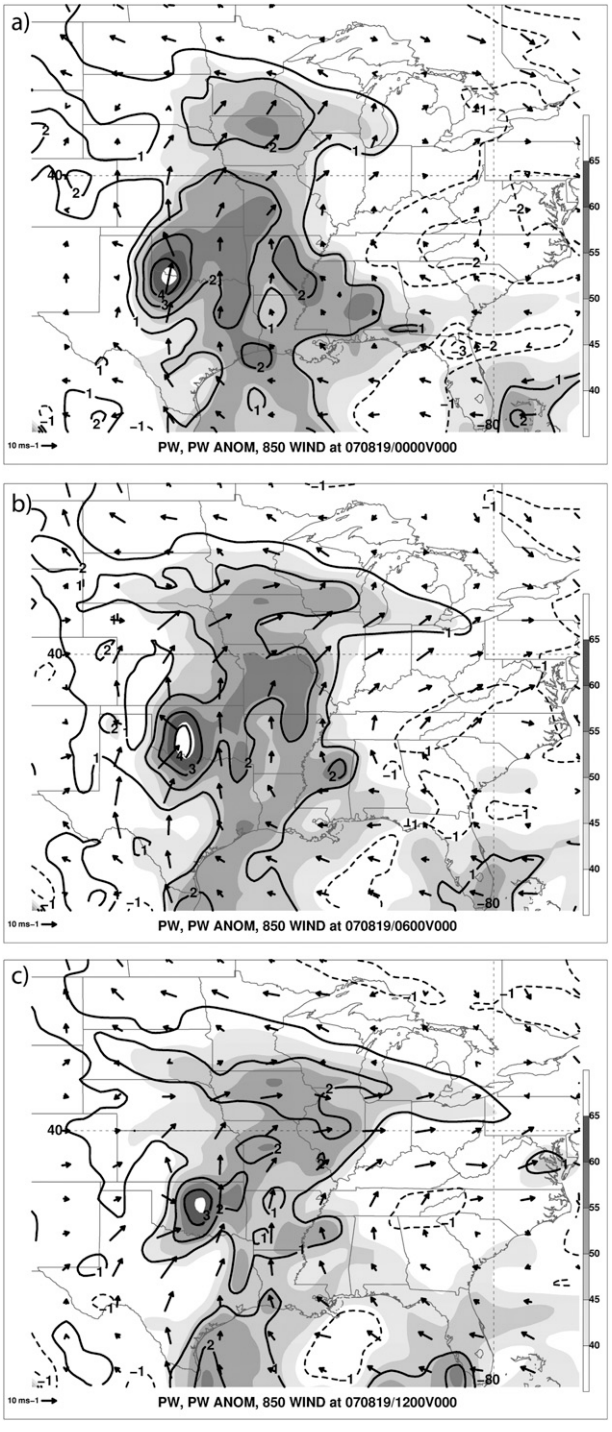

FIG. 3. PW (shaded in mm), 850-hPa wind vectors, and normalized anomalies of PW (contoured every 1 standard deviation with the zero contour removed) at (a) 0000, (b) 0600, and (c) 1200 UTC 19 Aug 2007. Fields shown are from the 1.0° GFS final analyses. Normalized anomalies were computed using the 21-day running long-term (1948–2008) mean and standard deviation, centered at the time of the analysis, from the NCEP–National Center for Atmospheric Research (NCAR) reanalysis (Kalnay et al. 1996), as in Hart and Grumm (2001).

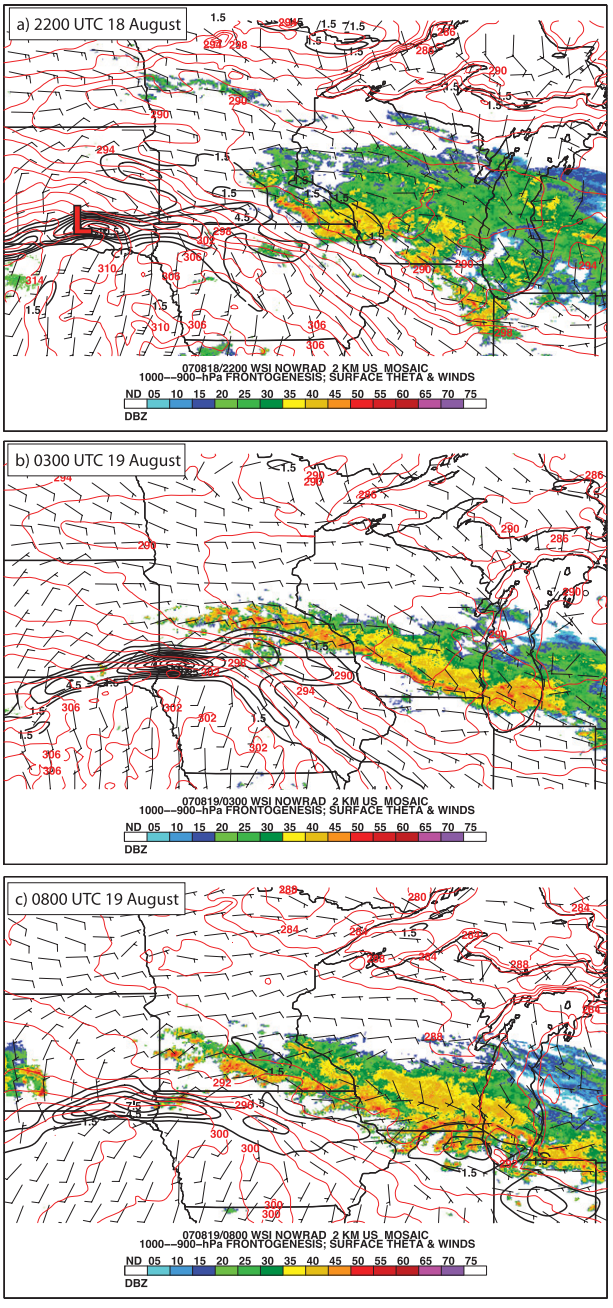

FIG. 4. Composite radar reflectivity [from the Weather Services International (WSI) NOWrad product] and Rapid Update Cycle (RUC; Benjamin et al. 2004) analysis of 2-m AGL potential temperature (red contours every 2 K), 10-m AGL winds (short barb = 2.5 m s^{-1}, long barb = 5 m s^{-1}, pennant = 25 m s^{-1}), and frontogenesis in the 1000–900-hPa layer [black contours every 1.5 K (100 km)$^{-1}$ (3 h)$^{-1}$ above 1.5] at (a) 2200 UTC 18 Aug, (b) 0300 UTC 19 Aug, and (c) 0800 UTC 19 Aug 2007. The location of the surface low-pressure center is marked with an "L" in (a).

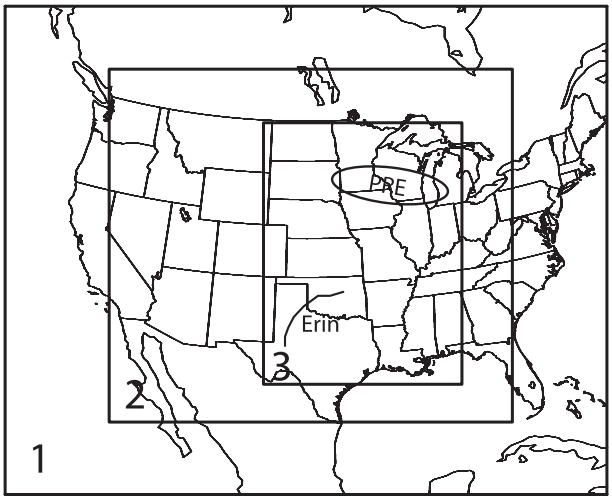

FIG. 5. Location of model domains. The horizontal grid spacing is 27 km on domain 1, 9 km on domain 2, and 3 km on domain 3. The observed track of TC Erin (after 0000 UTC 18 Aug) and the approximate location of the PRE are shown within domain 3.

3. Numerical simulation

a. *Model configuration*

To simulate the TC Erin PRE, version 3.0.1.1 of the Advanced Research Weather Research and Forecasting model (ARW-WRF; Skamarock et al. 2008) was integrated at convection-permitting grid spacing. In these simulations, the model was initialized at 0000 UTC 18 August 2007, which is approximately 24 h prior to the initiation of the PRE, and integrated for 42 h. This initialization time was chosen for several reasons. First, at 0000 UTC 18 August, the atmospheric moisture attributable to Erin was easy to distinguish from other moisture. Second, we wanted to capture the full process of moisture transport and initiation of convection after the model's spinup period. Third, it was necessary to consider both computational cost and the predictability of the situation: earlier initialization times might provide a more complete picture of the multiscale processes in this event, but they might also produce poorer simulations of the event. As will be discussed further below, the 0000 UTC 18 August initialization time was found to provide a good balance between lead time and simulation quality.

The National Centers for Environmental Prediction (NCEP) Global Forecast System (GFS) final analyses on a 1.0° latitude × 1.0° longitude grid were used as initial and lateral boundary conditions; the boundary conditions were updated every 6 h. The simulations used two-way grid nesting, with three grids at 27-, 9-, and 3-km horizontal spacing (Fig. 5). These grids were designed to include the Erin vortex, the poleward transport of moisture, and the

TABLE 1. Design of ARW-WRF version 3.0.1.1 numerical model experiments. Multiple entries indicate different configurations for domains 1, 2, and 3. See Fig. 5 for domain locations. Technical descriptions of the parameterizations are available online in Skamarock et al. (2008).

Parameter	Setting
Horizontal grid spacing (km)	27.0, 9.0, 3.0
Vertical levels	48, 48, 48
Time step (s)	108, 36, 12
Initial and boundary conditions	1.0° GFS
Cumulus convection	Kain (2004), Kain (2004), explicit
Boundary layer	Mellor–Yamada–Janjic
Surface layer	Monin–Obukhov (Eta)
Microphysics	Thompson, with two-moment rain
Land surface	Noah
Turbulence	2D Smagorinsky
Shortwave radiation	Dudhia (1989)
Longwave radiation	Rapid radiative transfer
Diffusion	Sixth-order monotonic (Knievel et al. 2007)
Scalar advection	Positive definite (Skamarock and Weisman 2009)

PRE MCS all on the innermost grid. A horizontal grid spacing of ~3 km with explicitly predicted convection can be expected to properly resolve convective systems, but individual convective elements are not well resolved (e.g., Weisman et al. 1997; Bryan et al. 2003; Schwartz et al. 2009). The vertical grid consisted of 48 levels and was stretched such that its finest grid spacing (approximately 100 m) was in the boundary layer and gradually became coarser with height to a maximum grid spacing of about 700 m near the model top at the 50-hPa level. Most of the parameterization schemes used in the simulations (Table 1) are similar to those often used in real-time applications of the ARW-WRF (e.g., Weisman et al. 2008). One relatively new parameterization that is used in this study is based on a bulk cloud microphysics parameterization described by Thompson et al. (2008), but with the prediction of the number concentration of raindrops (G. Thompson 2009, personal communication).

b. Overview of control run

Before moving on to the details of the control simulation, we must first establish that it provides a reasonable simulation of the structure of the MCS and its rainfall in Minnesota and Wisconsin. In the simulation, a northwest–southeast-oriented line of convection develops along the western edge of the stratiform rain region, much like what was observed (Fig. 6a). New development causes the line to expand westward and the MCS takes on the TL/AS pattern of organization and motion as well (Figs. 6b,c). However, the simulated convective line develops north and west of the location of the observed system (cf. Figs. 6 and 4). The surface baroclinic zone and associated frontogenesis are also displaced northward in the simulation; the observed thermal gradient at 0300 UTC was located along the Minnesota–Iowa border (Fig. 4b), whereas the simulated gradient had moved northward into southern Minnesota by this time (Fig. 6b). This suggests that the primary reason for the error in the position of convection is the error in the position of the low-level forcing for ascent.

The overall distribution of simulated precipitation is similar to observations (cf. Figs. 7 and 1), with a broad swath of >50 mm and embedded areas exceeding 200 mm. The maximum point total in the simulated PRE is 366 mm, compared with the observed maximum of 384 mm. Consistent with the simulation's displacement error for the MCS, however, is a northward and westward displacement of the simulated rainfall swath. The most extreme rainfall amounts in the model are located in west-central Minnesota, in contrast to the observed location in southeastern Minnesota and western Wisconsin. The spatial distribution and accumulations of rainfall associated with the remnants of TC Erin itself are also similar between the observations and simulation, but again the location is incorrect, this time to the southwest (cf. Figs. 7 and 1).

The perception of the quality of this simulation may vary depending on the perspective of the reader. As guidance to be used for predicting the potential flood response, it is probably not of much use, since the heaviest rain would have fallen on much different terrain than what happened in reality. This result is generally consistent with those of other forecasts and simulations with explicitly predicted convection, in that the model accurately captured the timing and convective mode, but not the exact location (e.g., Roebber et al. 2004; Kain et al. 2008; Weisman et al. 2008). However, because the simulation accurately represented the most important processes in the PRE—the organization and motion of convection, the widespread nature of the heavy rainfall, and the extreme local rainfall amounts—it is well suited

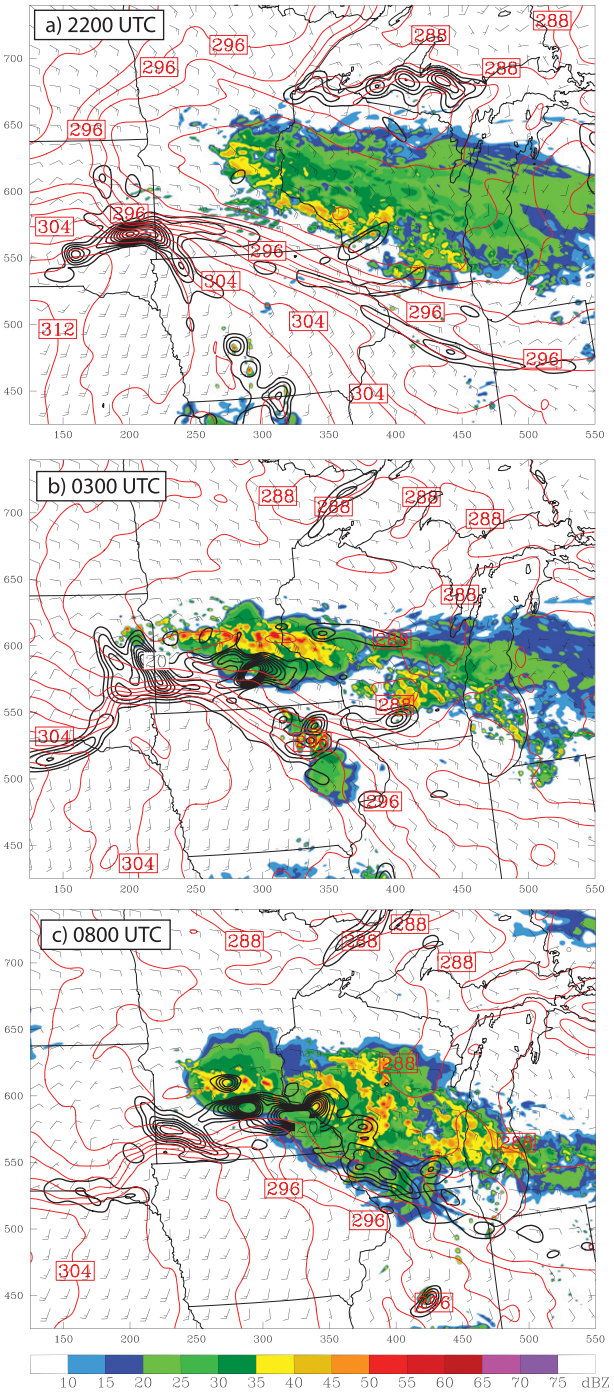

FIG. 6. As in Fig. 4, but for output from the control simulation on a portion of domain 3. Here, frontogenesis is averaged over the bottom five model layers (approximately the lowest 600 m AGL) and is contoured every 5 K (100 km)$^{-1}$ h^{-1} above 5. Note that frontogenesis in the model output is shown in units that are 3 times greater than those in the RUC analyses in Fig. 4, and that the simulated values are much larger. This is at least partially attributable to the higher spatial resolution, and the explicit representation of convective processes, in the model.

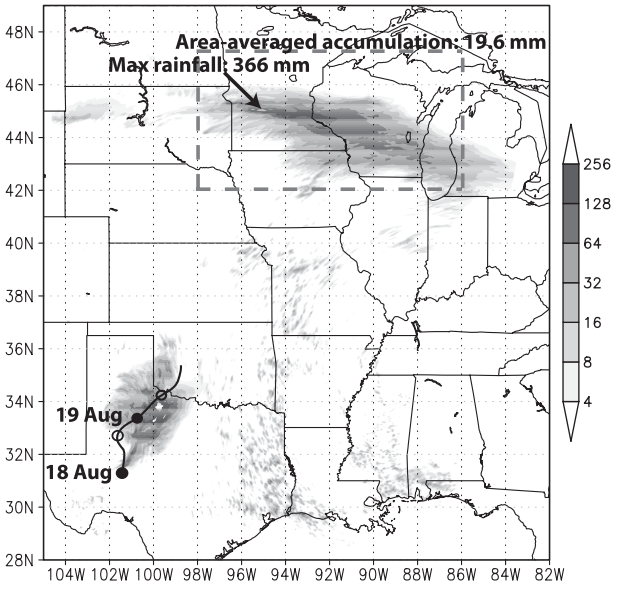

FIG. 7. As in Fig. 1, but for simulated rainfall on domain 3 of the control simulation. The gray dashed rectangle indicates the location of the area-average rainfall calculation. The approximate track of the simulated Erin vortex is shown.

for use as a control for quantifying the precipitation enhancement caused by tropical moisture transport ahead of TC Erin.

c. *Trajectories*

One method for establishing the sources of moisture for the MCS is by examining the trajectories of air parcels in the model output. GBS10 diagnosed backward parcel trajectories from GFS analyses and found that much of the air at the location of the MCS originated within the moisture plume brought onshore by Erin (see their Fig. 22). To augment this finding, forward trajectories starting at 850 hPa in Oklahoma, at the leading edge of the Erin-related moisture, were calculated from the output of our simulation (Fig. 8a). These trajectories illustrate the strong southerly low-level flow over the Great Plains on 18 August 2007, with the plume of high precipitable water also surging northward ahead of Erin (Figs. 8a,b). By 0600 UTC 19 August, many of these parcels have already risen in deep updrafts and turned eastward aloft (Figs. 8b and 9). Others have remained at low levels, with some having turned to the east, and others to the west, illustrating the strong deformation along the low-level baroclinic zone (Fig. 8b). These forward trajectories, in conjunction with the backward trajectories presented by GBS10, firmly establish that air originating in the Erin moisture plume on 18 August arrived in Minnesota and Wisconsin in time to participate in deep convection. What remains to be established, however, is exactly how important that moist air was in enhancing the convective rainfall.

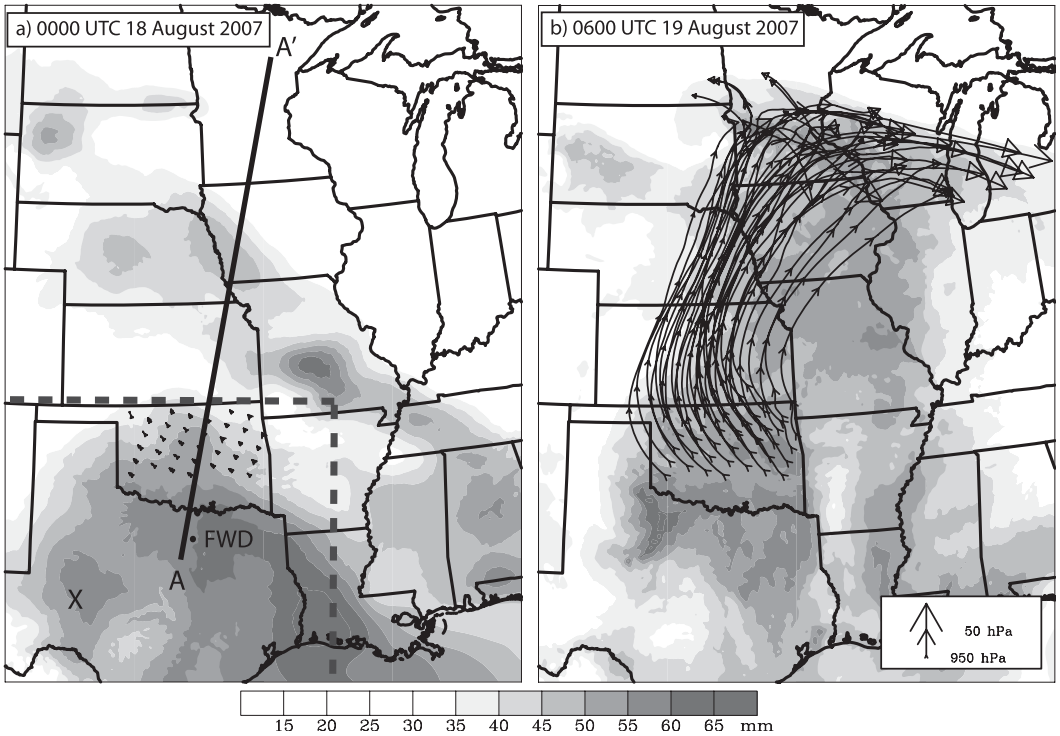

FIG. 8. (a) PW (mm) on domain 3 of the control simulation at the initialization time of 0000 UTC 18 Aug 2007, and the starting locations for forward trajectories; all of these trajectories were started at 850 hPa. (b)As in (a), but for 0600 UTC 19 Aug 2007. The positions of the forward trajectories at this time are shown with closed triangles; the arrows mark the trajectory positions every 6 h. The size of the arrowheads and triangles represent the pressure of the parcel, with larger arrowheads representing lower pressures (higher heights), according to the scale in the lower right. The location of the Erin vortex is shown by the ''X'' in (a). Also shown in (a) are dashed lines enclosing the box where the moisture reduction was applied for the NOPLUME simulation; see the text for details.

4. Sensitivity simulation

a. Method

To quantify the importance of Erin in the extreme rainfall in the Midwest, we sought to design a numerical sensitivity experiment in which the effects of Erin were removed. Because the remnants of Erin did not pass over the region where the extreme-rain-producing MCS occurred, it was not necessary to remove the Erin vortex. In fact, removing the vortex would be unlikely to have a substantial effect, because tropical moisture had already been brought onshore by the initialization time of 0000 UTC 18 August. This contrasts with the case studied by Wang et al. (2009), where the TC was very strong and both kinematic and moisture effects were important, and the TC needed to be removed to fully understand its importance. Instead, we chose to modify only the water vapor field in the initial conditions. The kinematic differences resulting from this choice will be addressed in section 4c.

To accomplish this, a latitude–longitude box was defined that separated the moisture owing to Erin from other regions of high PW (Fig. 8a). Then, at all horizontal and vertical grid points within this box where the relative humidity was greater than or equal to 55% in the initial conditions, the relative humidity was reduced to 55%. This modification, therefore, only reduced the atmospheric water vapor in places where it was already very moist; drier locations and locations where the moisture was unrelated to Erin were untouched. In the southern Plains and along the Gulf Coast, this resulted in PW values being reduced from 50–65 to 35–45 mm in most locations (Fig. 10), which is close to the climatological PW for this region.

The modification was only made in the initial conditions at 0000 UTC 18 August, approximately 24 h before the initiation of deep convection in Minnesota and Wisconsin. After this time, the simulation proceeds with no further modifications. As a result, this sensitivity experiment allows for a direct comparison between the control simulation (which was a reasonable replication of reality), and what might have happened had Erin not transported deep tropical moisture into the central United States. Hereafter, this sensitivity simulation will be referred to as ''NOPLUME,'' because the plume of tropical moisture associated with Erin has been removed.

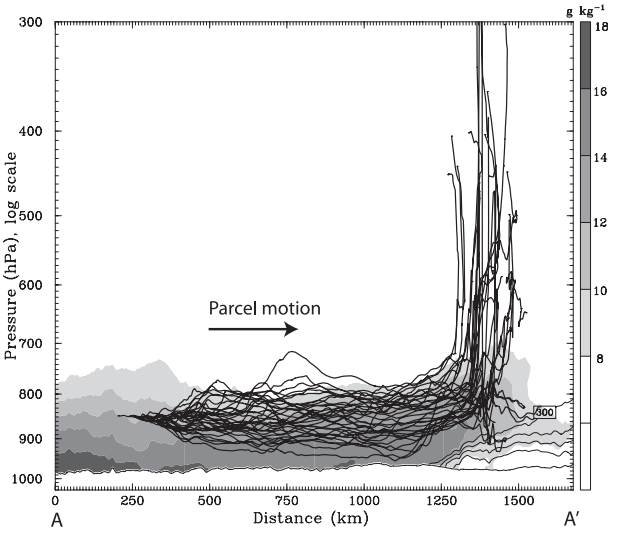

FIG. 9. South-southwest to north-northeast vertical section showing the parcel trajectories from Fig. 8b, along with the water vapor mixing ratio (g kg^{-1}; shaded) and potential temperature (thin contours every 3 K for values at and below 300 K; to show the location of the surface front and stable layer) at 0600 UTC 19 Aug. The mixing ratio and potential temperature values are averaged over 25 grid points (75 km) on either side of line A–A′ in Fig. 8a.

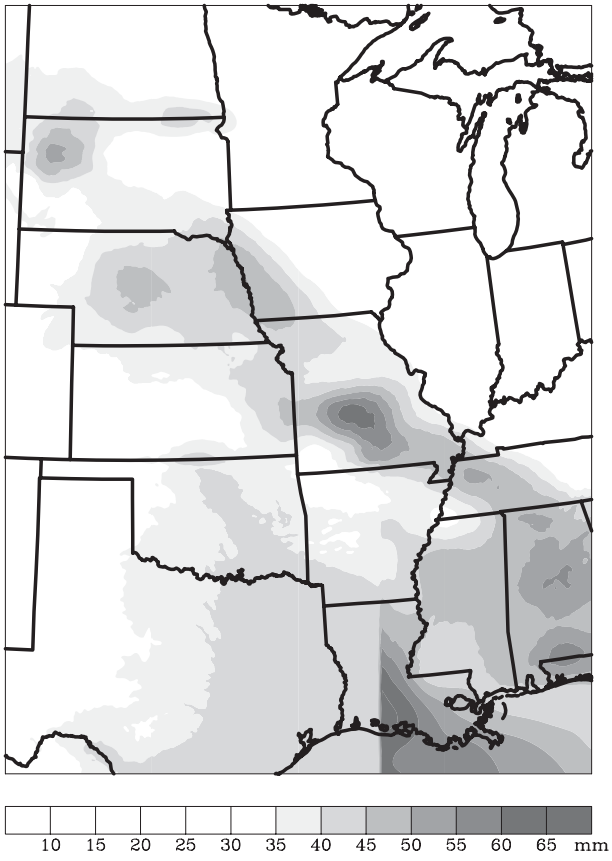

FIG. 10. As in Fig. 8a, but for the initial conditions of the NOPLUME simulation.

There are some potential limitations to this method. First, the use of a latitude–longitude box to apply the water vapor reduction did result in some discontinuities in the model's moisture fields (e.g., in central Louisiana in Fig. 10), but inspection of the model output at later times indicates that this gradient was removed by mixing within a few hours, and was not important to the simulated convection in the midwestern United States. Second, reducing the amount of water vapor in the sensitivity experiment also means that mass has been removed from the model's initial state. However, because the moisture was removed prior to generating the initial and boundary condition grid files for input into the model, hydrostatic balance was restored in that procedure prior to model integration. Dynamic balance is not restored in this procedure, but the results of McTaggart-Cowan et al. (2003) suggest that the effects of removing moisture on the initial wind field are likely to be negligible. One advantage to using a reduction in relative humidity for this type of sensitivity experiment is that the amount of water vapor remains tied to the temperature, and the thermal profile remains unchanged; however, we have not attempted to adjust for any changes in lapse rates that might have occurred in a drier environment. Finally, because we have only removed moisture and not the Erin vortex, our method does not account for any distant dynamical (as opposed to strictly thermodynamical) effects that the vortex, and its associated convection, may have caused. This issue will be addressed further in section 4c.

b. Comparison with control

In Fig. 11, the initial conditions in the control and NOPLUME simulations are compared with the observed sounding at Fort Worth, Texas, at 0000 UTC 18 August 2007. The initial conditions in the control simulation compare favorably with observations; both soundings have PW values slightly greater than 55 mm, and most unstable CAPE values exceeding 2000 J kg^{-1} (Figs. 11a,b). The sounding from NOPLUME still shows ample moisture through the atmospheric column, with a surface dewpoint temperature of 19°C and PW of 38.7 mm (Fig. 11c), but the values are greatly reduced from the anomalously moist conditions caused by Erin. The most unstable CAPE in NOPLUME is also greatly reduced, to less than 100 J kg^{-1}.

As discussed by GBS10, there were two primary regions with high PW at 0000 UTC 18 August: the plume of moisture associated with Erin in the southern plains, and a northwest–southeast-oriented region across the

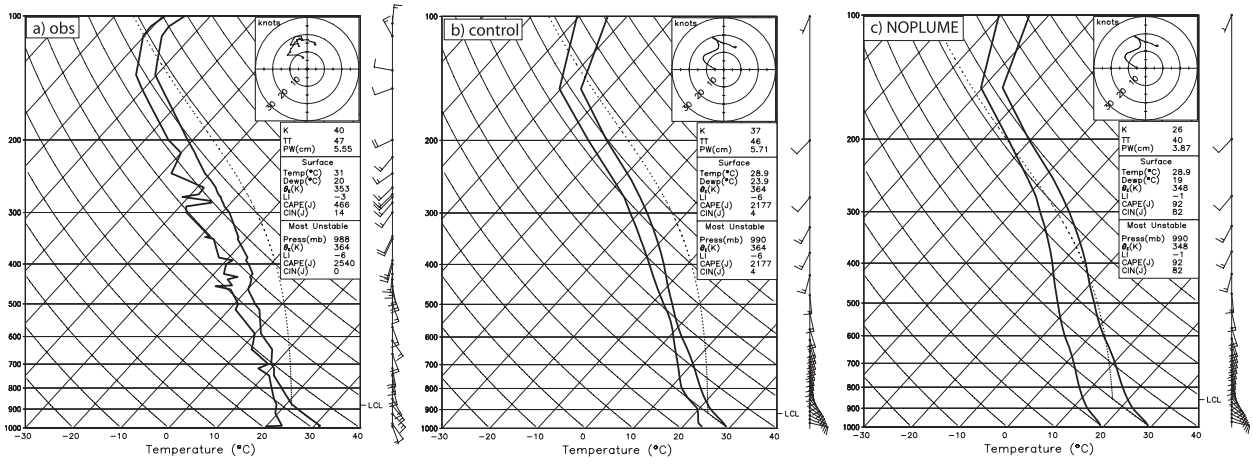

FIG. 11. Skew T–log$p$ diagrams and wind hodographs at 0000 UTC 18 Aug 2007. (a) Observed sounding from Fort Worth, TX (KFWD; location shown in Fig. 8a). (b) Sounding at same location from initial condition of the control simulation. (c) Sounding at same location from initial condition of the NOPLUME simulation. Parcel paths for the parcels with the highest θ_e in the lowest 3 km are shown by the dotted lines. The hodographs show the winds in the lowest 600 hPa of the atmosphere.

Great Plains and Mississippi Valley (Figs. 2 and 8a). Whereas the control simulation contains both of these regions of enhanced moisture, the NOPLUME simulation only has the latter (Fig. 10). In both simulations, high values of PW are transported northeastward by the strong low-level flow (Fig. 12). The PW increases and becomes concentrated in Minnesota and Wisconsin by 0000 UTC 19 August on the warm side of the west–east-oriented baroclinic zone (Figs. 12a,b,d,e). In the control simulation, the Erin-related moisture has almost merged with the ambient region of moisture by 0000 UTC (Fig. 12b), and the two PW maxima have merged by 0600 UTC (Fig. 12c), consistent with the observations and operational analyses shown in GBS10 (their Figs. 19d and 20). The NOPLUME simulation shows a maximum of PW in Minnesota and Wisconsin at 0600 UTC 19 August (Fig. 12f), but the high values of PW are confined mainly to that area; there is not a stream of high PW approaching it from the south as there is in the control. There are also some differences in the low-level flow between the two runs, which will be addressed in more detail in section 4c.

The difference in moisture transport between the two runs is also illustrated in hourly calculations of moisture flux across two west–east planes: one from southern Nebraska to northern Missouri and one from southern South Dakota to western Wisconsin (Fig. 13; location of planes is shown in Fig. 12a). The difference between the control and NOPLUME runs is particularly large at the southern location (Fig. 13b) after 2100 UTC 18 August, when the Erin-related moisture moved northward through the planes in the control run, but not in NOPLUME (Figs. 12b,e). Across the northern plane (Fig. 13a), the moisture flux is generally smaller during the time of the peak intensity of the MCS, as is the difference between the control and NOPLUME simulations. This is a result of the later arrival of the Erin-related moisture farther north, and because the water vapor field has a more diffuse structure at later times and in the northern part of the domain (Figs. 12c,f). The difference between the two runs is more pronounced in the boundary layer than at midlevels (Fig. 13), owing to both the higher water vapor mixing ratios in the boundary layer and to the greater initial reduction in boundary layer moisture that resulted from more areas with 55% or greater RH in the boundary layer than at midlevels at the initialization time.

Prior to the initiation of deep convection, the two simulations were nearly identical in their representations of the baroclinic zone and associated rain shield in the upper Midwest (cf. Figs. 6a and 14a). This agreement provides some justification for our method of designing the sensitivity experiment; it shows that the modification of the initial moisture conditions in the southern plains did not have spurious effects on the kinematic fields farther north prior to the arrival of the Erin-related moisture. As in the control simulation, deep convection initiates in NOPLUME after about 2200 UTC, and it organizes into a similar west–east-oriented line of training convective cells (Fig. 14b). However, this line is displaced slightly poleward of the line in the control simulation, and its convection is less intense and has a smaller region of stratiform precipitation associated with it. Between 0300 and 0800 UTC, the differences between the two simulations become even better defined, as new convective cells continue to develop on the western flank of the line in the control run, but this does not occur in NOPLUME. As a result, by 0800 UTC (Figs. 6c and 14c), there is still

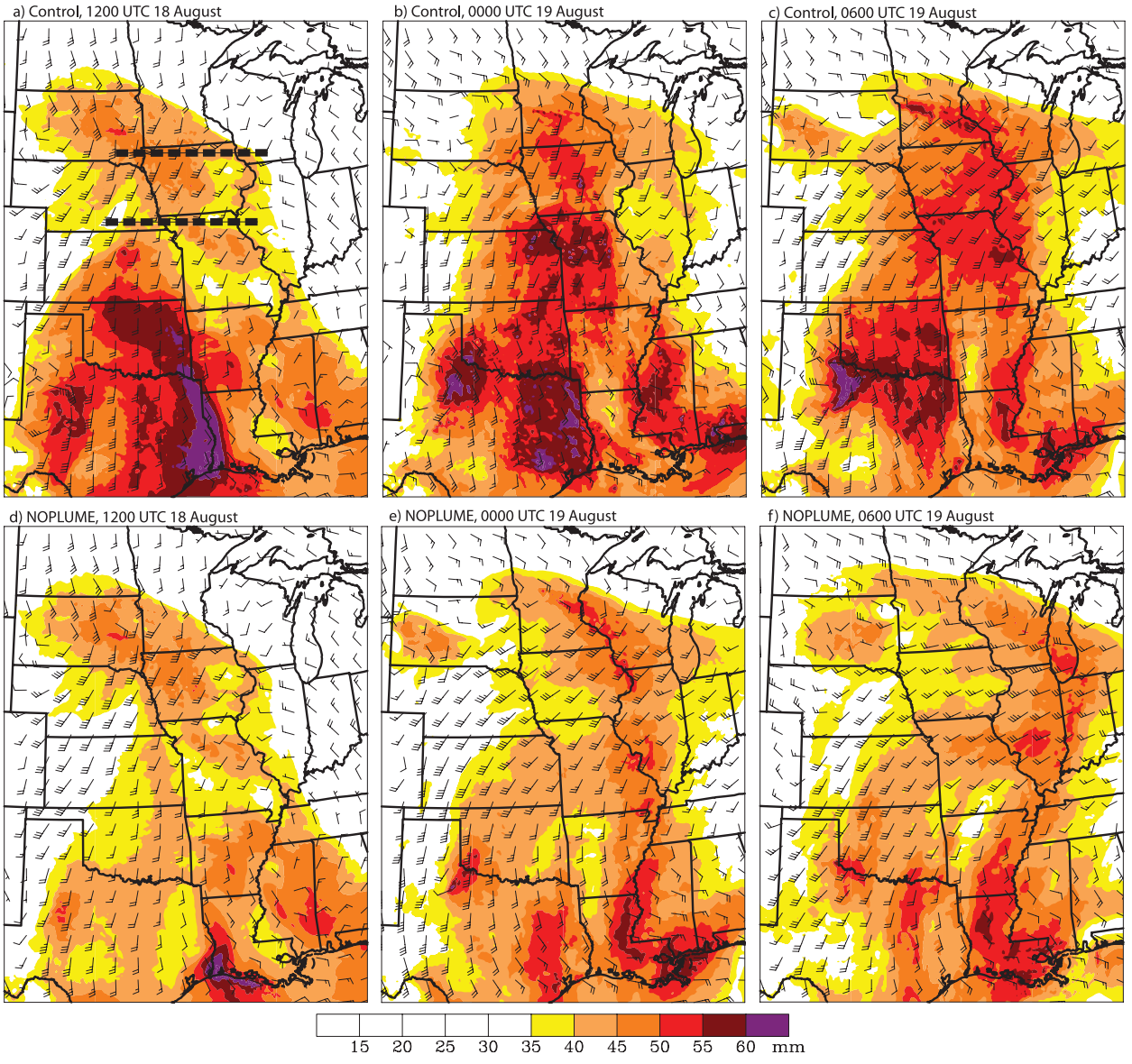

FIG. 12. PW (mm; shaded) and 850-hPa winds (short barb = 2.5 m s^{-1}, long barb = 5 m s^{-1}, pennant = 25 m s^{-1}) on domain 3 of (a),(b),(c) the control simulation and (d),(e),(f) the NOPLUME experiment. Times shown are (a),(d) 1200 UTC 18 Aug; (b),(e) 0000 UTC 19 Aug; and (c),(f) 0600 UTC 19 Aug 2007. The thick dashed lines in (a) show the locations of planes used for the calculations shown in Fig. 13.

a training line of convection in central Minnesota in the control, while the MCS has weakened and moved eastward into Wisconsin in the NOPLUME simulation. In other words, the back-building process takes place in the control run, but does not in NOPLUME.

Much of the reason for these differences in the maintenance of the MCS can be attributed to the poleward transport of moisture associated with Erin. As the convective line was initiating and organizing in both simulations at around 0000 UTC 19 August, there was a frontal surface that sloped upward from south to north (Figs. 15a,d). Air was being lifted as the strong southerly flow rose along the upward-sloping isentropes of this frontogenetic baroclinic zone, similar to past findings on the environments of elevated MCSs (e.g., Trier and Parsons 1993; Laing and Fritsch 2000; Moore et al. 2003). There was also an ample supply of elevated CAPE on the cool side of the surface front, and surface-based CAPE on the warm side, in both simulations, with values exceeding 2000 J kg^{-1} (Figs. 15a,d). As time progressed, more high-CAPE air in the boundary layer approached the front from the south, with much of it

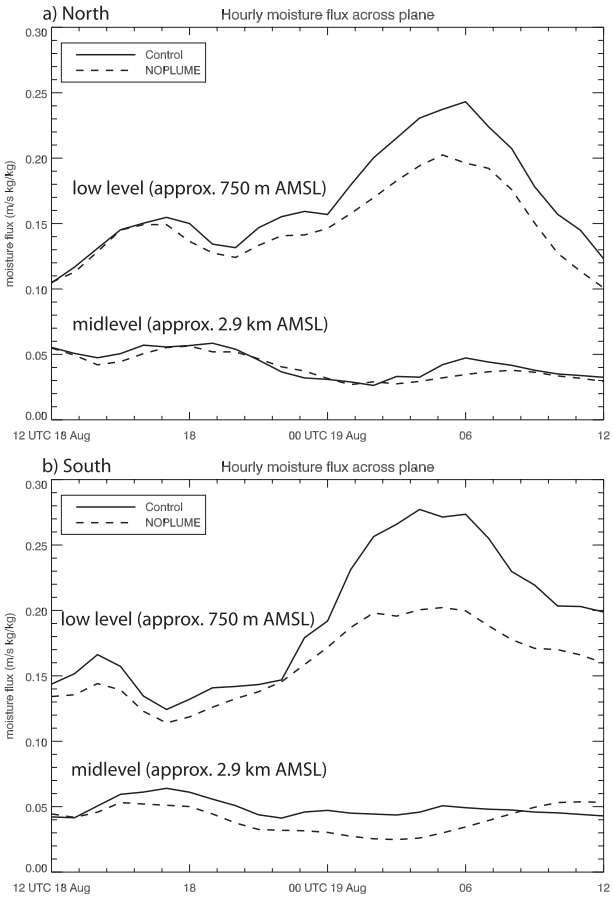

FIG. 13. Moisture flux (m s^{-1} kg kg^{-1}), calculated each hour, across (a) the northern plane and (b) the southern plane shown by the thick dashed lines in Fig. 12. Solid lines show the control simulation and dashed lines show NOPLUME. Values have been averaged along the full length of the plane. In both (a) and (b), the top curves are calculated on a model level approximately 750 m MSL, and the bottom curves are calculated on a level approximately 2.9 km MSL.

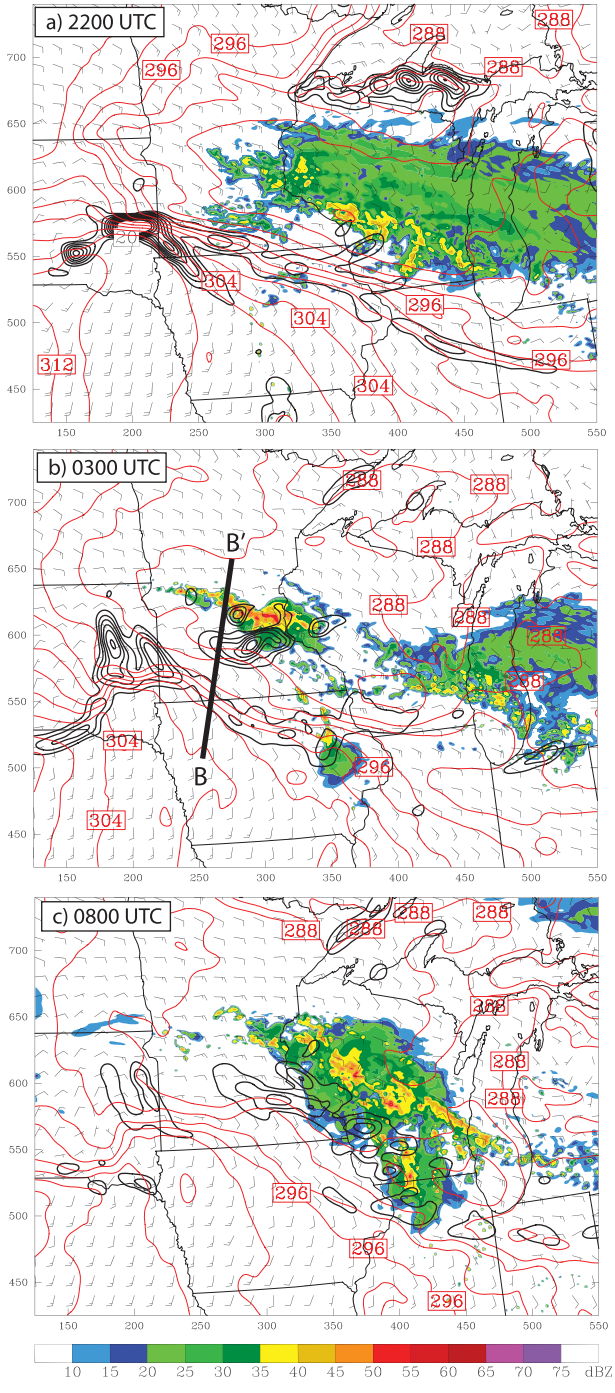

FIG. 14. As in Fig. 6, but for the NOPLUME simulation.

rising in deep convective updrafts and making up the linear MCS (Figs. 15b,e). This is where the differences between the two simulations—and the importance of the tropical moisture—become especially clear. In the control simulation, there is a seemingly unlimited supply of high-CAPE air to the south of the front (Figs. 15b,c), whereas the NOPLUME run has only a local source of moisture and CAPE (Figs. 15e,f). As a result, new convection continues to initiate on the western side of the MCS in the control, as moist air is transported into the area and is lifted along the sloping frontal surface. This allows the MCS as a whole to move slowly, and for more rainfall to accumulate at locations along the convective line. On the other hand, once the instability from nearby sources is released in the NOPLUME simulation, the development of new convective cells ceases and the MCS weakens. These results demonstrate that the lifting of warm, moist air along the baroclinic zone would have led to deep moist convection and a linear MCS regardless of whether Erin brought tropical moisture poleward, but that the tropical moisture plume provided an additional source of fuel for this MCS and allowed the

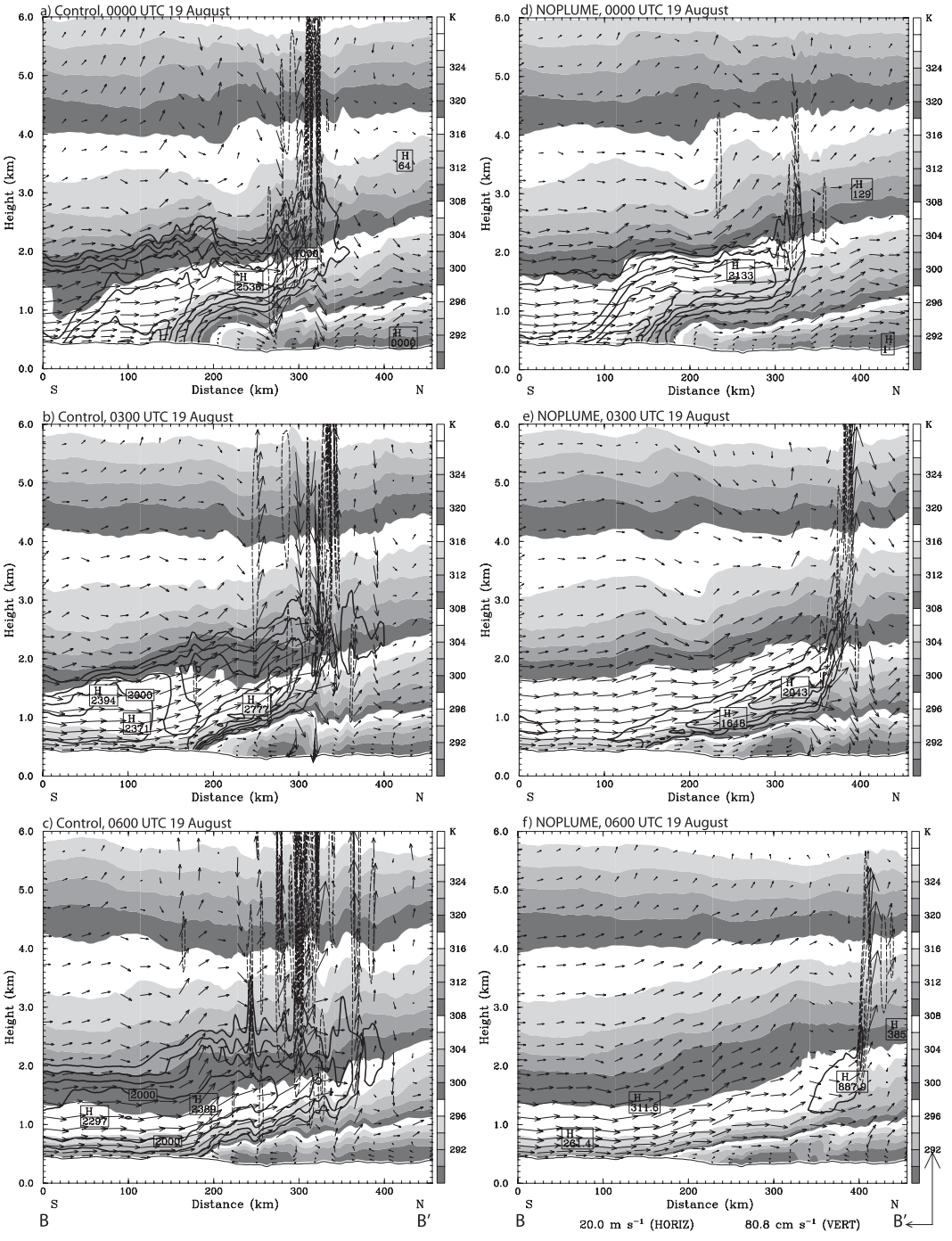

FIG. 15. South–north low-level vertical cross sections of potential temperature (shaded every 2 K), CAPE for parcels lifted from each level (contoured every 500 J kg^{-1} starting at 500), and flow vectors in the plane of the cross section (length scales shown at bottom; the scales for horizontal and vertical velocities are different) through line B–B′ shown on Fig. 14b. (a),(b),(c) From domain 3 of the control simulation and (d),(e),(f) from domain 3 of the NOPLUME simulation. Times shown are (a),(d) 0000 UTC 19 Aug; (b),(e) 0300 UTC 19 Aug; and (c),(f) 0600 UTC 19 Aug 2007. Values have been averaged over 3 grid points (9 km) on either side of the line.

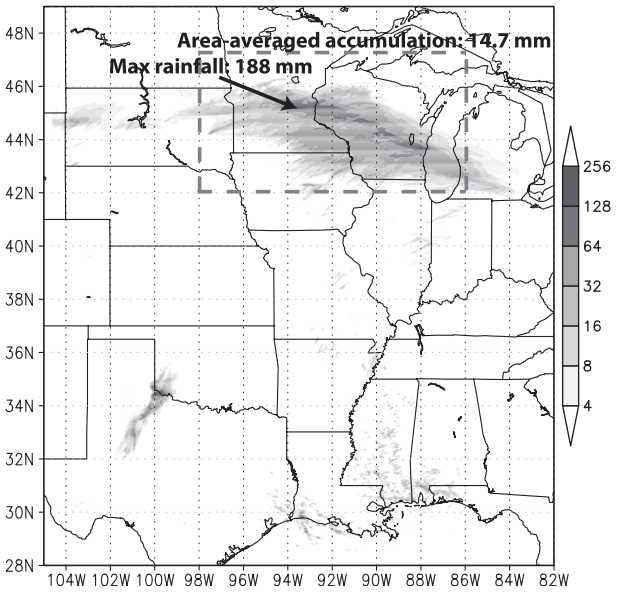

FIG. 16. As in Fig. 1, but for simulated rainfall on domain 3 of the NOPLUME simulation. The gray dashed rectangle indicates the location of the area-averaged rainfall calculation.

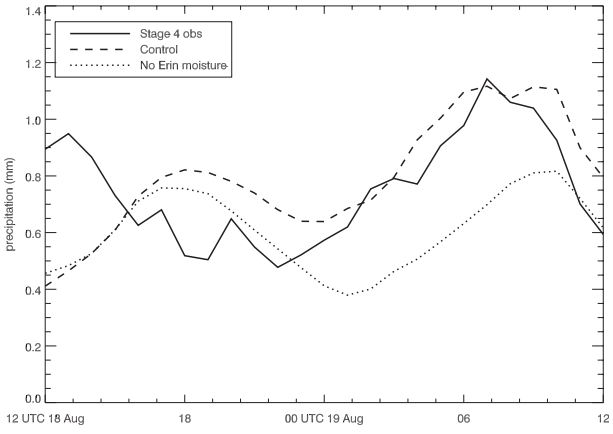

FIG. 17. Time series of hourly area averaged rainfall (mm), calculated over the PRE region shown by the gray dashed boxes in Figs. 1, 7, and 16. The solid line is from the stage-IV precipitation analysis, the dashed line is from the control simulation, and the dotted line is from the NOPLUME simulation.

deep convection to persist and to build westward for a longer period.

In total, this experiment reveals that the tropical moisture brought poleward by Erin caused a near doubling of the maximum rainfall amount from the MCS—the maximum 24-h total in the NOPLUME run was 188 mm compared with 366 mm in the control run and 384 in observations (cf. Figs. 1, 7, 16). The total 24-h area-averaged rainfall from the MCS was 19.6 mm in the control run (Fig. 7) and 14.7 mm in the NOPLUME run (Fig. 16), compared with 17.9 mm in the stage-IV analysis (Fig. 16). This represents an approximately 25% reduction in *total* rainfall from the control run to NOPLUME, or, in other terms, the Erin related moisture led to a 33% enhancement of the total rainfall. The greatest difference in the rainfall rate occurred during the MCS's mature stage between approximately 0000 and 1000 UTC 19 August (Fig. 17).

To place these results in context, the 188-mm peak accumulation in NOPLUME would exceed the 100-yr recurrence interval for 24-h precipitation in central Minnesota (Hershfield 1961). This emphasizes the fact that the synoptic and mesoscale environment was already very favorable for heavy rainfall. The additional moisture brought poleward ahead of Erin, and its enhancement of the deep convection over the Midwest, turned a notable rainfall event into an unprecedented 24-h rainfall event with an estimated recurrence interval for this amount of over 2000 yr (Minnesota State Climatology Office 2010).

c. *Kinematic influences*

As noted previously, the Erin vortex was not removed from the initial conditions, as the choice was made to focus on the effects of the tropical moisture in our experiments. However, because the near-surface circulation associated with Erin dissipates within about 12 h of the start of NOPLUME (not shown), and the overall vortex weakens considerably, it is possible that differences in the kinematics, in addition to moisture, are responsible for some of the differences in the MCS rainfall in the Midwest. For example, Lackmann (2002) showed that diabatic heating from convection can enhance the strength of LLJs in the warm sector of extratropical cyclones. Warm-core vortices also produce strong anticyclonic outflow aloft, which can increase the intensity of upper-level jets and ultimately effect synoptic and mesoscale vertical motions through quasigeostrophic forcing for ascent.

An examination of the upper-level kinematic differences between the two simulations at 0300 UTC, when the MCS is reaching its mature stage, shows that the most pronounced differences are in the environment surrounding the vortex, with some distant effects as well (Fig. 18). The most robust difference is in the 200-hPa winds on the periphery of Erin in Oklahoma and Kansas; in the control run, there is strong anticyclonic, divergent outflow aloft that is not present in the NOPLUME simulation (Fig. 18a). The 200-hPa winds are slightly stronger in NOPLUME in Minnesota and Wisconsin; otherwise, the upper-tropospheric flow in the vicinity of the MCS is very similar between the two runs. At low levels, the greatest differences are again near the Erin vortex itself, with strong winds and a strong vortex in the control, and weaker

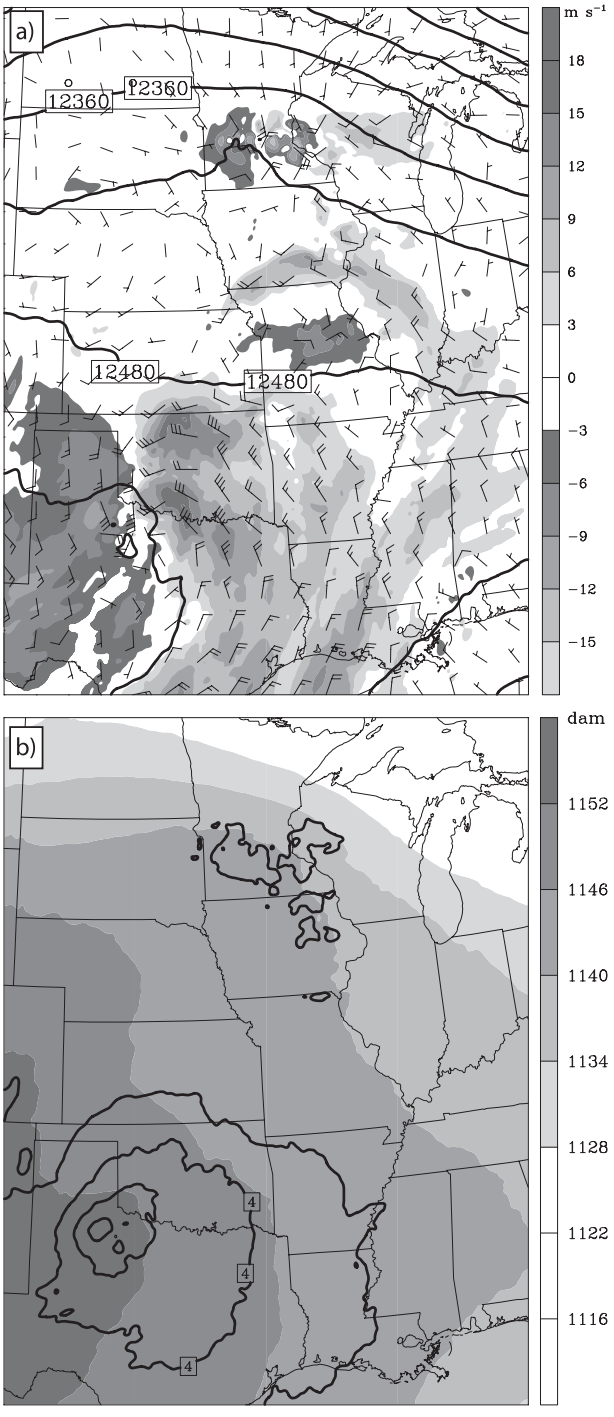

FIG. 18. Comparison of control and NOPLUME simulations at 0300 UTC 19 Aug. (a) 200-hPa geopotential height from the control simulation (contoured every 60 m), wind speed difference (shaded in m s^{-1}), and vector wind difference (short barb = 2.5 m s^{-1}, long barb = 5 m s^{-1}, pennant = 25 m s^{-1}) between the control and NOPLUME sensitivity simulations. (b) 900–200-hPa thickness (shaded in dam) from the control simulation and thickness difference between the control and NOPLUME simulations (contoured every 2 dam; zero contour omitted).

winds with the weaker vortex in NOPLUME (Fig. 19). The combination of greater cyclonic flow at low levels and anticyclonic flow aloft in the control run is consistent with the stronger warm core of the Erin vortex shown in Fig. 18b. There are also some changes in the strength and direction of the low-level jet (LLJ) in the upper Midwest, especially later in the simulation (Fig. 19). At 1800 UTC 18 August, the differences in the low-level winds in the upper Midwest between the two runs are small (Fig. 19a), but by 0300 UTC 19 August there is a broad region in Iowa and Wisconsin where the LLJ is approximately 2 m s^{-1} stronger in the control (Fig. 19b). The LLJ in the NOPLUME simulation also has more of a westerly component than does the control LLJ. This can be seen as easterly vector differences in Kansas and Nebraska in Fig. 19b, and by comparing the wind barbs in Figs. 12c,f.

These results show that in addition to the transport of moisture ahead of TC Erin, there were also some changes to the flow that may have affected the MCS in the Midwest. For example, the more southerly LLJ may have promoted back-building convection in Minnesota in the control run compared with NOPLUME. Because these differences at low levels primarily developed later in the simulation, they may also be a response to the stronger MCS, and greater instability, in the control simulation compared with NOPLUME. Fully attributing the cause and effect of these kinematic differences, however, would require additional numerical experiments that are beyond the scope of this study. Furthermore, the question of how the synoptic- and mesoscale environment might have evolved *had Erin never existed in the first place* remains unanswered, but is a possible avenue of future research using data from medium-range ensemble forecasts.

5. Conclusions

In this study, convection-permitting numerical simulations were used to quantify the enhancement of precipitation in a midlatitude convective system by the transport of deep tropical moisture ahead of a recurving TC. This high-impact predecessor rain event (PRE) ahead of TC Erin brought record rainfall and deadly flooding in Minnesota and Wisconsin. A control simulation provided a reasonable replication of the observed event, with a simulated maximum rainfall amount of 366 mm, compared with the observed maximum of 384 mm. The overall distribution of rainfall also compared favorably with observations, although the swath of heaviest precipitation was displaced slightly to the north in the simulation relative to observations. Furthermore, the organization and motion of the extreme-rain-producing MCS were very similar to what was observed, and were similar to previously

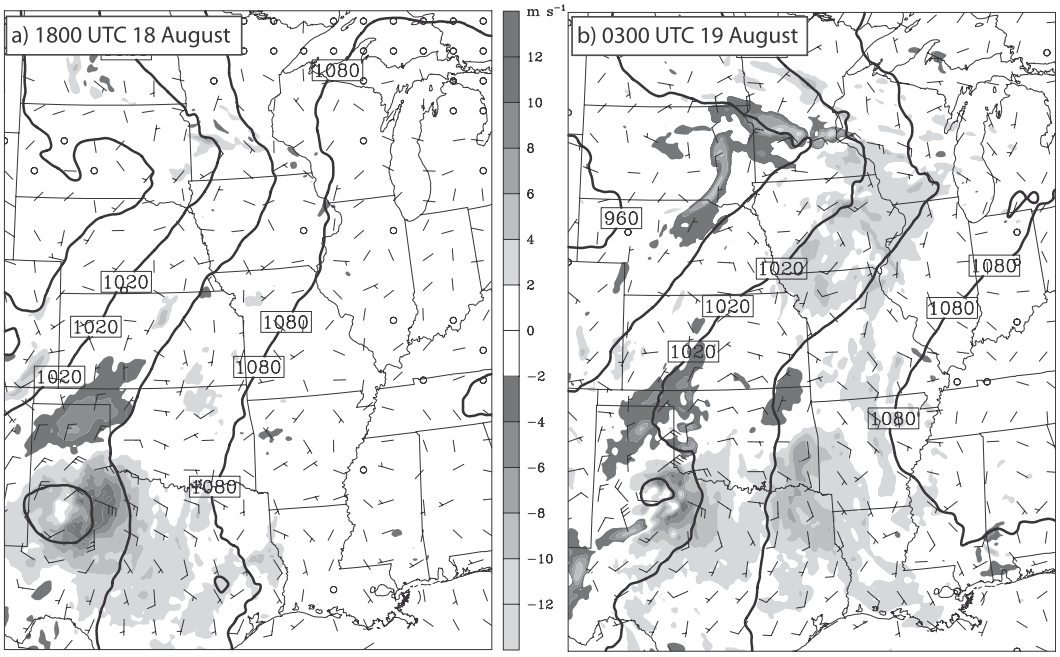

FIG. 19. 900-hPa geopotential height from the control simulation (contoured every 30 m), wind speed difference (shaded in m s^{-1}), and vector wind difference (short barb = 2.5 m s^{-1}, long barb = 5 m s^{-1}, pennant = 25 m s^{-1}) between the control and NOPLUME sensitivity simulations at (a) 1800 UTC 18 Aug and (b) 0300 UTC 19 Aug 2007.

documented instances of elevated, linear convective systems that occur on the cool side of a surface boundary.

The effects of the tropical moisture were examined using both parcel trajectories and a sensitivity experiment. The trajectories revealed that air originating within the Erin-related tropical moisture plume arrived in the inflow region of the simulated MCS as it was organizing and intensifying. In the sensitivity experiment, referred to as NOPLUME, the water vapor associated with Erin was removed from the model's initial conditions. In this simulation, an MCS developed and initially had similar characteristics to that in the control run. This suggests that, even without any influence from Erin, the synoptic- and mesoscale conditions were favorable for a heavy-rain-producing linear MCS along the low-level baroclinic zone. However, the MCS in the NOPLUME simulation did not persist as long as the MCS in the control run, nor did convection continue to build on the MCS's western flank. This was attributed to the limited supply of moisture south of the baroclinic zone. In the control run, both the ambient water vapor in the Midwest, plus the moisture from Erin, allowed high-CAPE air to flow into the system for an extended period. In the NOPLUME run, only the ambient moisture and CAPE was available, and once this CAPE was released, the MCS weakened and moved eastward.

In total, the maximum rainfall amount in NOPLUME was approximately half of that in the control run, and there was a 25% decrease in the area-integrated precipitation. Or, to address the question of how much additional rain fell as a result of Erin-related moisture, our results show that it caused a near doubling of the maximum precipitation amount, and a 33% increase in the area-integrated precipitation. This enhancement transformed this event from a notable rainfall event to an unprecedented one.

This study represents the beginning of an effort to quantify the distant effects of recurving TCs on midlatitude precipitation systems in the United States. The TC Erin PRE was an ideal candidate for this type of analysis because the TC remnants did not pass over the heavy rainfall area, allowing for a simpler separation of the moisture sources. Other methods are currently being used to better understand the physical and dynamical processes relevant to, and the predictability of, PREs. These methods include removing the TC from the initial conditions prior to landfall (e.g., Wang et al. 2009), and using ensemble sensitivity techniques (e.g., Hakim and Torn 2008) to analyze precipitation forecasts from ensemble members that did and did not have PREs. These efforts are aimed at improved understanding, and ultimately forecasting, of these high-impact heavy rain events.

Acknowledgments. Computing resources for running the simulations were provided by the National Center

for Atmospheric Research. WSI NOWrad data were also provided by NCAR, and RUC analyses were provided by the National Climatic Data Center. The authors thank Stan Trier, Morris Weisman, and Christopher Davis for helpful discussions and suggestions regarding this work, and Greg Thompson for providing code for his microphysics parameterization. The authors also thank Ron McTaggart-Cowan and an anonymous reviewer for numerous helpful suggestions that led to an improved manuscript. Galarneau and Bosart were supported by NSF Grant ATM-0553017, and Galarneau's contribution to this research was also supported by an NCAR Advanced Study Program Graduate Student Visitor Fellowship during the 2009 spring semester. Schumacher was partially supported by National Science Foundation Grant AGS-0954908.

REFERENCES

Arndt, D. S., J. B. Basara, R. A. McPherson, B. G. Illston, G. D. McManus, and D. B. Demko, 2009: Observations of the overland reintensification of Tropical Storm Erin (2007). *Bull. Amer. Meteor. Soc.,* **90,** 1079–1093.

Augustine, J. A., and F. Caracena, 1994: Lower-tropospheric precursors to nocturnal MCS development over the central United States. *Wea. Forecasting,* **9,** 116–135.

Benjamin, S. G., and Coauthors, 2004: An hourly assimilation–forecast cycle: The RUC. *Mon. Wea. Rev.,* **132,** 495–518.

Binau, S., 2009: The historic flash flood event of 18–19 August 2007 in the Upper Mississippi River Valley: Impacts of terrain and societal response. *Extended Abstracts, 23rd Conf. on Weather Analysis and Forecasting/19th Conf. on Numerical Weather Prediction,* Omaha, NE, Amer. Meteor. Soc., 1B.4. [Available online at http://ams.confex.com/ams/pdfpapers/154238.pdf.]

Bosart, L. F., and F. H. Carr, 1978: A case study of excessive rainfall centered around Wellsville, New York, 20–21 June 1972. *Mon. Wea. Rev.,* **106,** 348–362.

——, and G. M. Lackmann, 1995: Postlandfall tropical cyclone reintensification in a weakly baroclinic environment: A case study of Hurricane David (September 1979). *Mon. Wea. Rev.,* **123,** 3268–3291.

Brennan, M. J., R. D. Knabb, M. Mainelli, and T. B. Kimberlain, 2009: Atlantic hurricane season of 2007. *Mon. Wea. Rev.,* **137,** 4061–4088.

Bryan, G. H., J. C. Wyngaard, and J. M. Fritsch, 2003: Resolution requirements for the simulation of deep moist convection. *Mon. Wea. Rev.,* **131,** 2394–2416.

Chappell, C. F., 1986: Quasi-stationary convective events. *Mesoscale Meteorology and Forecasting,* P. S. Ray, Ed., Amer. Meteor. Soc., 289–309.

Corfidi, S. F., 2003: Cold pools and MCS propagation: Forecasting the motion of downwind-developing MCSs. *Wea. Forecasting,* **18,** 997–1017.

Doswell, C. A., III, H. E. Brooks, and R. A. Maddox, 1996: Flash flood forecasting: An ingredients-based methodology. *Wea. Forecasting,* **11,** 560–581.

Dudhia, J., 1989: Numerical study of convection observed during the Winter Monsoon Experiment using a mesoscale two-dimensional model. *J. Atmos. Sci.,* **46,** 3077–3107.

Fritsch, J. M., R. J. Kane, and C. R. Chelius, 1986: The contribution of mesoscale convective weather systems to the warm-season precipitation in the United States. *J. Climate Appl. Meteor.,* **25,** 1333–1345.

Galarneau, T. J., Jr., L. F. Bosart, and R. S. Schumacher, 2010: Predecessor rain events ahead of tropical cyclones. *Mon. Wea. Rev.,* **138,** 3272–3297.

Hakim, G. J., and R. D. Torn, 2008: Ensemble synoptic analysis. *Synoptic-Dynamic Meteorology and Weather Analysis and Forecasting: A Tribute to Fred Sanders, Meteor. Monogr.,* No. 55, Amer. Meteor. Soc., 147–161.

Hart, R. E., and R. H. Grumm, 2001: Using normalized climatological anomalies to rank synoptic-scale events objectively. *Mon. Wea. Rev.,* **129,** 2426–2442.

Hershfield, D. M., 1961: Rainfall frequency atlas of the United States for durations from 30 minutes to 24 hours and return periods from 10 to 100 years. U. S. Weather Bureau Tech. Paper 40, 115 pp. [NTIS PB-88237961.]

Junker, N. W., R. S. Schneider, and S. L. Fauver, 1999: A study of heavy rainfall events during the Great Midwest Flood of 1993. *Wea. Forecasting,* **14,** 701–712.

Kain, J. S., 2004: The Kain–Fritsch convective parameterization: An update. *J. Appl. Meteor.,* **43,** 170–181.

——, and Coauthors, 2008: Some practical considerations regarding horizontal resolution in the first generation of operational convection-allowing NWP. *Wea. Forecasting,* **23,** 931–952.

Kalnay, E., and Coauthors, 1996: The NCEP/NCAR 40-Year Reanalysis Project. *Bull. Amer. Meteor. Soc.,* **77,** 437–471.

Knievel, J. C., G. H. Bryan, and J. P. Hacker, 2007: Explicit numerical diffusion in the WRF model. *Mon. Wea. Rev.,* **135,** 3803–3824.

Lackmann, G. M., 2002: Cold-frontal potential vorticity maxima, the low-level jet, and moisture transport in extratropical cyclones. *Mon. Wea. Rev.,* **130,** 59–74.

Laing, A. G., and J. M. Fritsch, 2000: The large-scale environments of the global populations of mesoscale convective complexes. *Mon. Wea. Rev.,* **128,** 2756–2776.

Lin, Y., and K. E. Mitchell, 2005: The NCEP stage II/IV hourly precipitation analyses: Development and applications. Preprints, *19th Conf. on Hydrology,* San Diego, CA, Amer. Meteor. Soc., 1.2. [Available online at http://ams.confex.com/ams/pdfpapers/83847.pdf.]

Maddox, R. A., C. F. Chappell, and L. R. Hoxit, 1979: Synoptic and meso-α-scale aspects of flash flood events. *Bull. Amer. Meteor. Soc.,* **60,** 115–123.

McTaggart-Cowan, R., J. R. Gyakum, and M. K. Yau, 2003: Moist component potential vorticity. *J. Atmos. Sci.,* **60,** 166–177.

Minnesota State Climatology Office, cited 2010: Heavy rains fall on southeastern Minnesota: August 18–20, 2007. [Available online at http://climate.umn.edu/doc/journal/flash_floods/ff070820.htm.]

Moore, J. T., F. H. Glass, C. E. Graves, S. M. Rochette, and M. J. Singer, 2003: The environment of warm-season elevated thunderstorms associated with heavy rainfall over the central United States. *Wea. Forecasting,* **18,** 861–878.

NCDC, 2007: *Storm Data*. Vol. 49, No. 8, 530 pp.

Roebber, P. J., D. M. Schultz, B. A. Colle, and D. J. Stensrud, 2004: Toward improved prediction: High-resolution and ensemble modeling systems in operations. *Wea. Forecasting,* **19,** 936–949.

Schumacher, R. S., and R. H. Johnson, 2005: Organization and environmental properties of extreme-rain-producing mesoscale convective systems. *Mon. Wea. Rev.,* **133,** 961–976.

——, and ——, 2006: Characteristics of U.S. extreme rain events during 1999–2003. *Wea. Forecasting,* **21,** 69–85.

——, and ——, 2009: Quasi-stationary, extreme-rain-producing convective systems associated with midlevel cyclonic circulations. *Wea. Forecasting,* **24,** 555–574.

Schwartz, C. S., and Coauthors, 2009: Next-day convection-allowing WRF model guidance: A second look at 2-km versus 4-km grid spacing. *Mon. Wea. Rev.,* **137,** 3351–3372.

Skamarock, W. C., and M. L. Weisman, 2009: The impact of positive-definite moisture transport on NWP precipitation forecasts. *Mon. Wea. Rev.,* **137,** 488–494.

——, and Coauthors, 2008: A description of the Advanced Research WRF version 3. NCAR Tech. Note NCAR/TN-475+STR, 125 pp. [Available online at http://www.mmm.ucar.edu/wrf/users/docs/arw_v3.pdf.]

Stohl, A., C. Forster, and H. Sodemann, 2008: Remote sources of water vapor forming precipitation on the Norwegian west coast at 60°N—A tale of hurricanes and an atmospheric river. *J. Geophys. Res.,* **113,** D05102, doi:10.1029/2007JD009006.

Thompson, G., P. R. Field, R. M. Rasmussen, and W. D. Hall, 2008: Explicit forecasts of winter precipitation using an improved bulk microphysics scheme. Part II: Implementation of a new snow parameterization. *Mon. Wea. Rev.,* **136,** 5095–5115.

Trier, S. B., and D. B. Parsons, 1993: Evolution of environmental conditions preceding the development of a nocturnal mesoscale convective complex. *Mon. Wea. Rev.,* **121,** 1078–1098.

Uccellini, L. W., and D. R. Johnson, 1979: The coupling of upper and lower tropospheric jet streaks and implications for the development of severe convective storms. *Mon. Wea. Rev.,* **107,** 682–703.

Wang, Y., Y. Wang, and H. Fudeyasu, 2009: The role of Typhoon Songda (2004) in producing distantly located heavy rainfall in Japan. *Mon. Wea. Rev.,* **137,** 3699–3716.

Weisman, M. L., W. C. Skamarock, and J. B. Klemp, 1997: The resolution dependence of explicitly modeled convective systems. *Mon. Wea. Rev.,* **125,** 527–548.

——, C. Davis, W. Wang, K. W. Manning, and J. B. Klemp, 2008: Experiences with 0–36-h explicit convective forecasts with the WRF-ARW model. *Wea. Forecasting,* **23,** 407–437.

Zhu, Y., and R. E. Newell, 1998: A proposed algorithm for moisture fluxes from atmospheric rivers. *Mon. Wea. Rev.,* **126,** 725–735.